Dielectric and relaxor behavior of BaBi$_4$Ti$_4$O$_{15}$ ceramics

J.D. Bobić [a], M.M. Vijatović [a], S. Greičius [b], J. Banys [b], B.D. Stojanović [a,*]

[a] *Institute for Multidisciplinary Researches, Kneza Viseslava 1, 11000 Belgrade, Serbia*
[b] *Faculty of Physics, Vilnius University, 9 Sauletekio str., 10222 Vilnius, Lithuania*

ARTICLE INFO

ABSTRACT

Barium bismuth titanate BaBi$_4$Ti$_4$O$_{15}$ (BBiT) ceramics have been prepared using non-conventional solid-state reaction route based on mechanochemical synthesis during intensive milling. The X-ray diffraction method was used to determine phase composition. Dielectric properties were investigated in a wide range of temperatures (20–800 °C) and frequencies (1.21 kHz–1 MHz). The broad dielectric constant peaks at temperature T_m is frequently dependent. A modified Curie–Weiss relationship is used to study the diffuseness behavior of a ferroelectric phase transition where value of γ indicates the degree of diffuseness of barium bismuth titanate ceramics. The dielectric relaxation rate follows the Vogel–Fulcher relation with $E_a = 0.013$ eV, $\nu_0 = 2.09 \times 10^8$ Hz and $T_f = 651$ K. All these parameters indicate that BaBi$_4$Ti$_4$O$_{15}$ is a relaxor ferroelectric. Ohmic conductivities and associated activation energies were evaluated using impedance spectroscopy.

© 2010 Elsevier B.V. All rights reserved.

1. Introduction

The family of bismuth oxides was discovered more than 50 years ago by Aurivillius [1]. Recently, interest in the properties of the Aurivillius phases as temperature-stable ferro-piezoelectrics has been renewed. Several bismuth-layered crystal structures and their properties have been investigated in detail. The majority of those materials are normal ferroelectrics with a fairly high Curie temperature, while only a few of them such as BaBi$_2$Nb$_2$O$_9$, BaBi$_2$Ta$_2$O$_9$, etc. exhibit relaxor behavior [2–4]. Relaxor materials are characterized by frequency dispersion having broad dielectric anomaly near the dielectric maximum. The latter properties are very useful for a wide range of applications due to their extremely high dielectric and piezoelectric responses in a wide range of temperatures [5]. The most investigated relaxor ferroelectrics are Pb-based perovskites such as lead magnesium niobate (PMN), lanthanum-doped lead zirconate titanate (PLZT) and Pb-based complex perovskites such as Pb(Mg$_{1/3}$Nb$_{2/3}$O)$_3$-PbTiO$_3$ (PMN-PT) [6–8]. However, these materials have a disadvantage due to toxicity of lead. Therefore, there is a growing need for new lead-free materials for various applications such as Bi-based Aurivillius family of oxides. BaBi$_4$Ti$_4$O$_{15}$ (BBiT) as a member of this large family of compounds is a promising candidate for high-temperature piezoelectric applications, memory application and ferroelectric nonvolatile memories (Fe-RAM) but a lot of aspects of the preparation and properties of barium bismuth titanate remain unexplored.

The lattice structure of the Aurivillius family of compounds is composed of n number of like perovskite $(A_{n-1}B_nO_{3n+3})^{2-}$ unit cells sandwiched between $(Bi_2O_2)^{2+}$ slabs along pseudo tetragonal c-axis (n is an integer between 1 and 5). The 12 coordinate perovskite-like A-site is typically occupied by a large cation such as Na$^+$, K$^+$, Ca^{2+}, Sr^{2+}, Ba^{2+}, Pb^{2+}, Bi^{3+} or Ln^{3+} and the 6-coordinate perovskite-like B-site by smaller cations such as Fe^{3+}, Cr^{3+}, Ti^{4+}, Nb^{5+} or W^{6+}. BBiT, as the $n = 4$ member of the Aurivillius family has Ba and Bi ions at the A sites and Ti ions at the B sites of the perovskite block $[(Bi_2O_2)^{2+}\cdot((BaBi_2)Ti_4O_{13})^{2-}]$ [1].

The literature data shows that BBiT powders can be prepared by chemical and solid-state reaction methods. Most frequently used chemical methods are the polymeric precursors-Pechini process [9], sol–gel [10], co-precipitation [11] and templated grain growth (TGG) method [12]. There are many reports of the preparation of BBiT powders by conventional solid-state reaction starting from BaCO$_3$, TiO$_2$ and Bi$_2$O$_3$ that involve high temperature and time of calcination multi-steps [13–16].

A wide range of materials with Bi-based Aurivillius-type structure has been derived from mechanical assisted synthesis. That is a novel technique in which mechanical energy is supplied to the starting precursors by means of vigorous milling (mechanical activation). The influence of mechanical activation on the formation of some Aurivillius-type structure ceramics such as Bi$_4$Ti$_3$O$_{12}$ (BiT), and ABi$_4$Ti$_4$O$_{15}$ compounds, A = Ca, Sr, Ba, was investigated by several authors. Nanocrystalline BiT powders of high phase purity were obtained by intensive mechanical activation of starting oxides during milling in high-energy ball mill for 6 h by B. Stojanovic et al. and 9 h by Han and Ko [17,18]. Synthesis and characterization of SrBi$_4$Ti$_4$O$_{15}$ (SBiT) and CaBi$_4$Ti$_4$O$_{15}$ (CBiT) from oxide precursors via

high-energy mechanical activation are reported by Wang and co-workers [19,20]. Single phase CBiT and SBiT with nano-meter size are directly synthesized from their oxide mixtures (mechanochemical synthesis) after milling in high-energy shaker mill for 30 and 20 h, respectively. In contrast to the results reported by Wang et al [19,20], Castro and co-workers [21,22] intended to produce SBiT by milling using vibrating and planetary mill. After 168 h of milling in vibrating mill and 108 h in planetary mill there is no mechanosynthesis in either of the two milling processes. However, they reported that heating times and temperature can be reduced when staring with a precursor which has previously been mechanically activated.

In 2009, group of authors published results to preparation of $BaBi_4Ti_4O_{15}$ precursor using barium titanate ($BiTiO_3$) and bismuth titanate ($Bi_4Ti_3O_{12}$) powders obtained via mechanochemical synthesis after which these two powders were homogenized. The obtained mixture was used for preparing BBiT ceramics. However, there are no details about the preparation of BBiT in powder form [23,24]. According to our knowledge, there has been no report about synthesis of BBiT powder by solid-state reaction where starting oxides mixture was previously mechanically activated.

In this work, we analyzed synthesis of BBiT powders by solid-state reaction using mechanically activated mixed oxides: BaO, TiO_2 and Bi_2O_3. Mechanical activation enables high reactivity of the obtained powder mixture and favors processing with improvement in the electrical properties. The BBiT powder produced after mechanosynthesis exhibited a certain level of crystallinity but to obtain higher crystallinity, the calcination step was introduced. The influence of mechanical activation on time and temperature of thermal treatment was noticed. The dielectric and relaxor behavior of BBiT ceramics was also reported.

2. Experimental procedures

Stoichiometric amounts of high purity (Alfa Aesar, p.a. 99%) oxides: BaO, TiO_2 and Bi_2O_3, were milled for 20, 60, 180 and 360 min. The milling conditions were: zirconium oxide jars and zirconium oxide balls (d = 10 mm), ball-to-powder weight ratio was 20:1, basic disc rotation speed was 320 min^{-1} and rotation speed of discs with jars was ∼400 rpm. Mechanochemical activation was performed in the air atmosphere in a planetary ball mill (Fritsch Pulverisette 5). The obtained powder was calcinated at 750 °C for 4 h and pressed into pallets using a cold isostatic press (8 mm in diameter and ∼3 mm thick). Ceramic samples were prepared by conventional sintering of uniaxial pressed pellets (298 MPa) at 1130 °C for 1 h (Lenton-UK oven) in sealed alumina crucibles to avoid bismuth loss. The heating rate was 10 °C/min, with natural cooling in the air atmosphere. The density was calculated from the measurement of sample size parameters and weight. The relative density of the pellet was determined to be ∼92%.

The formation of phase and crystal structure of BBiT ceramics were verified using a conventional X-ray diffractometer (XRD, Model D5000, Siemens) with CuKα radiation ($\lambda_{K\alpha1}$ = 1.5405 Å, $\lambda_{K\alpha2}$ = 1.5443 Å, $I_{K\alpha1}/I_{K\alpha2}$ = 0.5), 2θ range between 10° and 80°, step size of 0.02° (2θ), divergence slit = 0.5 mm, receiving slit = 0.3 mm. The morphology and microstructure of the obtained ceramics were examined using a scanning electron microscope (SEM, Tescan VEGA TS 5130MM). The sintered samples for microstructure examination were polished to thickness of 1 mm with silicon carbide and alumina powder and cleaned in an ultrasonic bath in ethanol. The ceramic pellets for electrical measurement were painted by platinum on both sides, and fired at 750 °C to form electrodes. The electrical measurement of sintered samples (dielectric constant, dielectric losses and impedance) was measured using a HP 4284A in the 1.21 kHz–1 MHz frequency range and the temperature interval from 32 to 777 °C.

3. Results and discussion

The solid-state reactions initiated by intensive milling in high-energy ball mills could be a good choice for the ceramic powder preparation. The highly dispersed phase materials are formed during intensive milling (mechanical activation) and in some cases the formation of a new product can appear, due to solid-state reaction (mechanochemical synthesis) [25]. Even though the effect of energy exchange during high-energy milling is not completely clear, it has an efficient contribution to physical and in same cases chemical changes in starting materials. The result is a new material with a
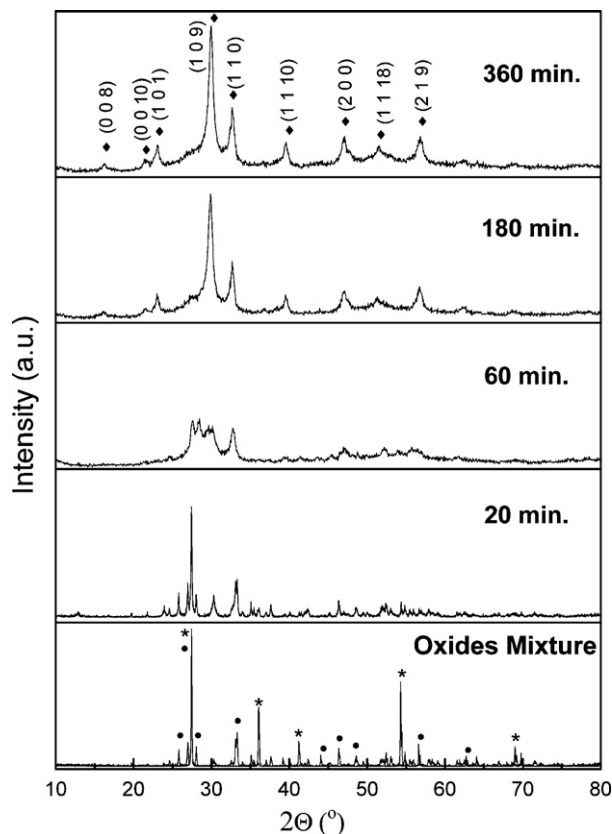
Fig. 1. XRD traces of homogenized starting oxide mixture of BaO, Bi_2O_3 and TiO_2 together with those mechanically activated for various time; (*) TiO_2; (●) Bi_2O_3; (♦) BBiT).

completely different structure and properties. As a consequence, solid-state reaction that normally requires high temperatures can occur at lower temperatures during milling, without any externally applied heat. Intensive milling increases the contact area between the reactant powder particles due to the reduction of particle size, thus allowing fresh surface to come into contact. During the formation of a new surface, the increase of the energy in surface layers occurs. In view of the above, in our case intensive milling in high-energy ball mills was used to initiate a solid-state reaction between the starting oxide components. Fig. 1 shows the XRD traces of homogenized starting oxide mixture of BaO, Bi_2O_3 and TiO_2 together with those mechanically activated for 20, 60, 180 and 360 min, respectively. Sharp peaks of crystalline Bi_2O_3 and TiO_2 are observed in the starting oxides mixture. No BaO is detected, as the amount added is rather small. Upon 20 min of mechanical activation, XRD peaks of the oxides start to be broad. The disappearance of sharp peaks for oxides and subsequent formation of broadened peaks suggest that a significant refinement in particle and crystallite size, together with a degree of amorphization of mixed oxides have taken place after 60 min of milling. For the composition mechanically activated for 180 and 360 min, diffraction peaks at 2θ angles of 16.9°, 21.2°, 23.1°, 30.0°, 32.7°, 39.3°, 47.0°, 51.5°, 56.8° are established. They correspond to BBiT (0 0 8), (0 0 10), (1 0 1), (1 0 9), (1 1), (1 1 10), (2 0 0), (1 1 18) and (2 1 9) planes, respectively, of the layered perovskite phase. No significant change in XRD pattern was observed when the milling time was increased to 360 min. The BBiT phase was formed after 360 min of intensive milling and further investigation was correlated with thermal treatment of the obtained powder. The calcination temperature and time was significantly reduced (750 °C for 4 h) comparing to the previously reported literature data (950 °C/12 h and 1050 °C/12 h; 1050 °C/5 h; 1050 °C/5 h twice) [13–16].
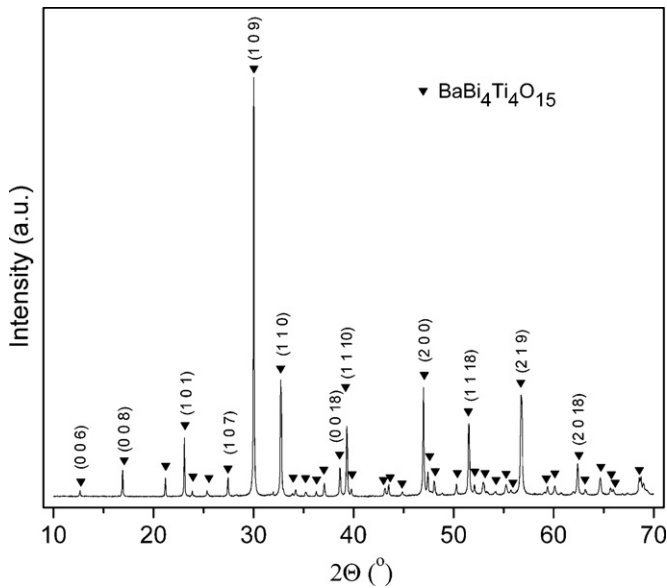
Fig. 2. X-ray diffraction pattern of BBiT ceramic sintered at 1130 °C for 1 h.

Fig. 2 shows the XRD patterns of BBiT ceramics obtained after sintering at 1130 °C for 1 h and could be indexed to a bismuth-layered perovskite structure with $n = 4$. No impurity peaks corresponding to the reactant oxides or any other secondary phases were found. The X-ray diffraction pattern can be well fitted to a tetragonal BBiT structure ($a = 0.3863$ nm, $c = 4.9997$ nm, JCPDS 35-0757), with non-polar space group $I4/mmm$. Aurivillius originally described BBiT as being tetragonal [1]. However, some authors using the both the synchrotron X-ray and neutron diffraction patterns [2,26,27] have suggested that the structure is in fact orthorhombic. The reflections indicative of orthorhombic symmetry are associated with the tilting of the TiO_6 octahedra. The difference between the macroscopic (tetragonal $I4/mmm$) and microscopic symmetry (orthorhombic $A2_1am$) might be due to the polarization fluctuation between allowable directions within (a, b) plane.

Microstructures of sintered samples of BBiT (Fig. 3) show plate like grains with a random orientation of plate faces. Plate like grain formation is known to be a typical characteristic of bismuth-layer-structured ferroelect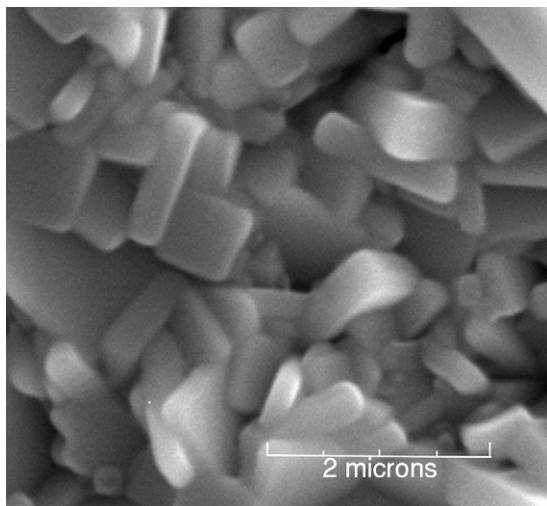rics as they have a highly anisotropic crystal structure. The plate like grains of BBiT ceramics have rounded edges up to 1 μm in length and up to 0.2 μm thickness.

Fig. 4 displays the dielectric constant (ε) and loss tangent (tan δ) as a function of temperature determined during cooling in BBiT ceramics measured in a frequency interval from 1.21 kHz to 1 MHz. As the frequency increased, the dielectric maximum shifted to a higher temperature (from 660 to 678 K) and the dielectric constant became smaller (from 2458 to 1951). The degree of relaxation behavior, obtained by $\Delta T_{relaxor} = T_{m(1.21MHz)} - T_{m(1kHz)}$ is found to be only 18 K which suggests that the shift of T_m with frequency is not much districted in BBiT ceramics. The loss tangent (tan δ) is very low at a room temperature (about 0.03) and almost constant from the room temperature to 200 °C and thereafter increases with temperature.

It is a well-known fact that the dielectric constant of a normal ferroelectric follows the Curie–Weiss law which is described by the relation:

$$1/\varepsilon = \left(\frac{(T - T_c)}{C} \right) \tag{1}$$

where T_c is the Curie temperature and C is the Curie constant. The Curie–Weiss plot between $1/\varepsilon$ and temperature gives a straight line with a slope of ($1/C$) and the X-axis intercept at T_c. The Curie–Weiss plot for BBiT ceramics at 100 kHz is shown in Fig. 5. The parameter ΔT_m which describes the degree of the deviation from Curie–Weiss law, is defined as:

$$\Delta T_m = T_{cw} - T_m \tag{2}$$

where T_{cw} denotes the temperature from which the permittivity starts to deviate from Curie–Weiss law and T_m represents the temperature of the dielectric maximum. Table 1 shows that ΔT_m increases with increasing frequency.

The broadness in ε_r versus temperature curve is one of the most important characteristics of the disordered perovskite structures showing relaxor behavior. A modified Curie–Weiss relationship is used to study the diffuseness behavior of a ferroelectric phase transition, given as [28]:

$$\frac{1}{\varepsilon} - \frac{1}{\varepsilon_{max}} = \frac{(T - T_{max})\gamma}{C}, \text{ for } (T > T_{max}) \tag{3}$$

where C is the modified Curie–Weiss constant and the value of γ ($1 \leq \gamma \leq 2$) indicates the degree of diffuseness of the material. In the case of "normal" ferroelectrics $\gamma = 1$, and $\gamma = 2$ for relaxors which corresponds to polar domains fluctuations in the neighborhood of
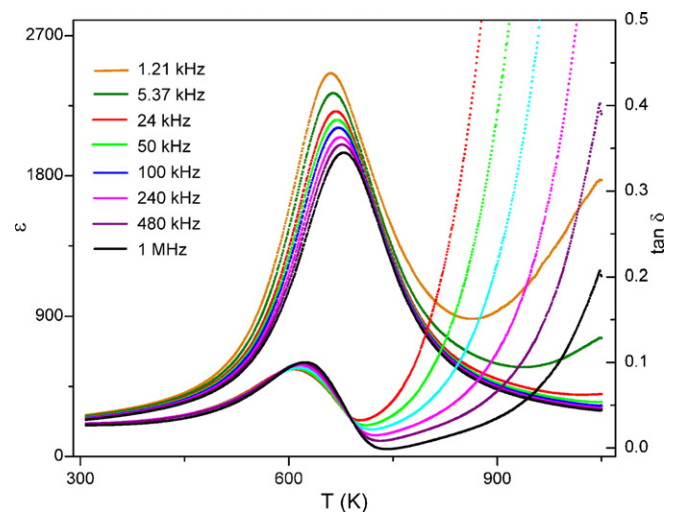

Fig. 3. SEM micrograph pattern of BBiT ceramics sintered at 1130 °C for 1 h.

Fig. 4. Temperature dependence of dielectric constant (ε) and loss tangent (tan δ) of BBiT ceramics at various frequencies.

Table 1
Some relaxor parameters of BBiT ceramic at different frequencies.

Frequency (kHz)	ε_{m}	T_{m} (K)	T_{c} (K)	T_{cw} (K)	ΔT_{m} (K)	ΔT_{relax} (K)
1.21	2458	660	674	722	63	18
100	2109	671	692	766	95	
1000	1951	678	699	780	102	
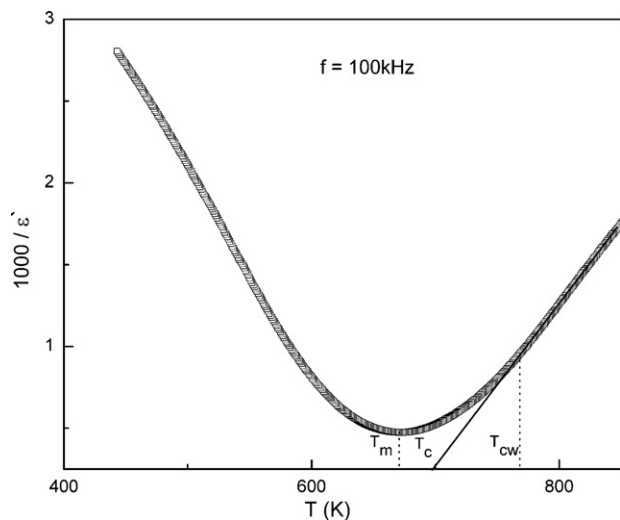
Fig. 5. The inverse dielectric constant ($1000/\varepsilon$) as a function of temperature at 100 kHz. (the dotted line represents the experimental data and the solid line is the fit to the Curie–Weiss law).

the maximum permittivity. A plot of $\ln(\varepsilon_{max}/\varepsilon - 1)$ as a function of $\ln(T - T_{max})$ at 100 kHz is presented on Fig. 6. The value of γ calculated from the slot of the curve is found to be 1.88 which reveals the near-relaxor nature of BBiT ceramics.

An empirical Vogel–Fulcher relationship [29] is used to account the dielectric relaxation nature in relaxor ferroelectrics. The variation of frequency of *ac* field with T_{m} is given as:

$$\nu = \nu_0 \exp\left\{ \frac{-E_a}{k_B(T_m - T_f)} \right\} \tag{4}$$

where ν_0 is the Debye frequency, E_a is the activation energy (i.e., the energy barrier between two equivalent polarization states), k_B is the Boltzmann's constant, T_f is the static freezing temperature of the

polarization fluctuations (i.e., the temperature at which dynamic reorientation of the dipolar cluster polarization can no longer be thermally activated). The variation of temperature of the dielectric maximum T_m as a function of $\ln(\nu)$ is presented on Fig. 7. From non-linear fitting of experimental data, the values were determined: $E_a = 0.013$ eV, $\nu_0 = 2.09 \times 10^8$ Hz, and $T_f = 651$ K. The temperature of the dielectric peak T_m shows a good fit to the Vogel–Fulcher law, indicating relaxor behavior. One of the accepted models to explain the relaxor behavior is based on the existence of compositional heterogeneity (different types of cations randomly occupying the same lattice of unit cell). According to that, it is considered that relaxor behavior of BBiT could attribute to the disorder of Ba^{2+} from perovskite slabs $((BaBi_2)Ti_4O_{13})^{2-}$ with Bi^{3+} from the $(Bi_2O_2)^{2+}$ layer.

The impedance data taken over a wide frequencies range at various temperatures as a Nyquist diagram (complex impedance spectrum) is presented on Fig. 8. The impedance characteristics of insulating ceramics are assumed to be composed of three components: grain, grain boundaries and sample/electrode interfaces. In the present investigations, only a single semicircle with a high frequency side passing through the origin is observed in the 700–1050 K temperature range. Therefore, the semicircle can be ascribed to the grain component for all investigated temperatures. At the higher temperatures (Fig. 8a), along with the semicircle a small tail is present in the low frequency side which could indicate the electrode-grain interface which serves as a trap for space charges. Similar behavior was observed for BBiT ceramics obtained by conventional solid-state reaction [13]. No such tail was observed at temperatures lower than 900 K (Fig. 8b). Ohmic conductivity was estimated from the bulk resistance R, which is derived by fitting the complex impedance data to an equivalent circuit model of a resistor and capacitor in parallel.

In BBiT the main contribution to the electrical conductivity at high temperatures generally originates from the thermally activated oxygen vacancies [30]. The temperature dependence of
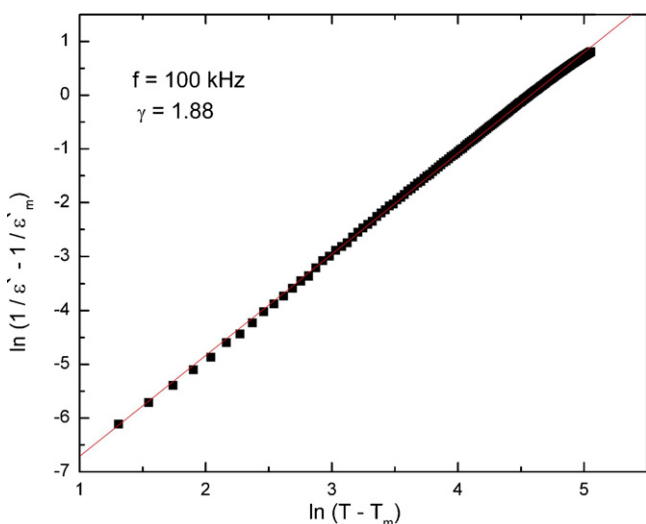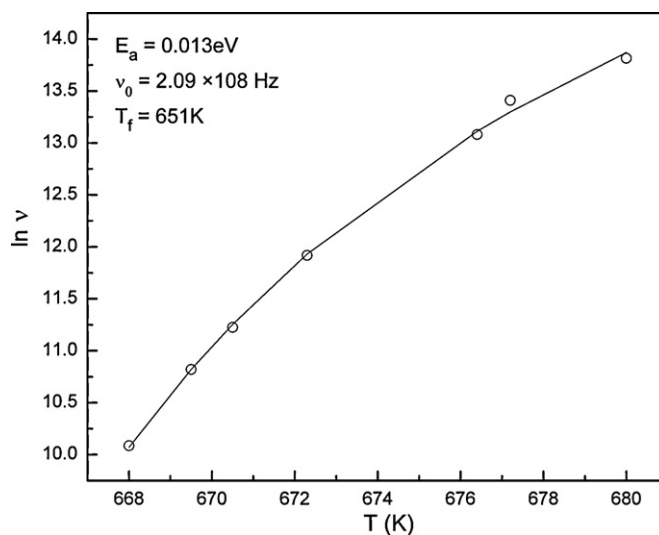

Fig. 6. $\ln(\varepsilon_{max}/\varepsilon - 1)$ as a function of $\ln(T - T_{max})$ at 100 kHz for BBiT ceramics (The dotted line represents the experimental data and solid line is the fit to Eq. (3)).

Fig. 7. Temperature of the dielectric maximum T_m as a function of $\ln(\nu)$ for the BBiT ceramics (the square dots represent the experimental data and the solid line is the fit to the Vogel–Fulcher relation).
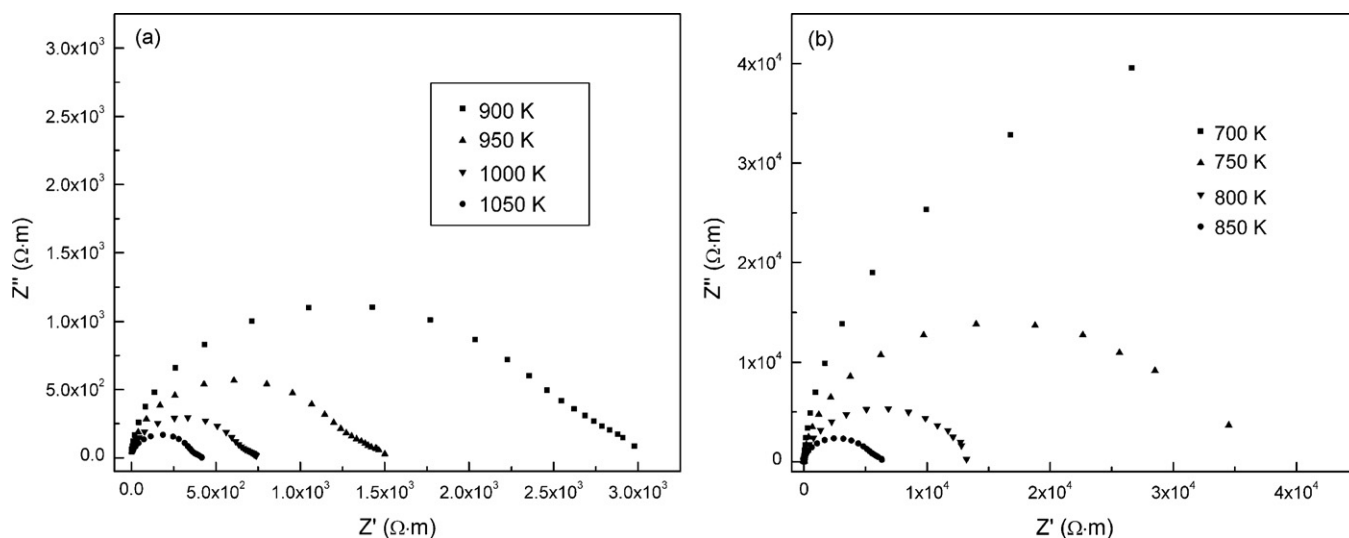
Fig. 8. Complex impedance plot of BBiT ceramics at different temperatures (a) 900–1050 K and (b) 700–850 K.
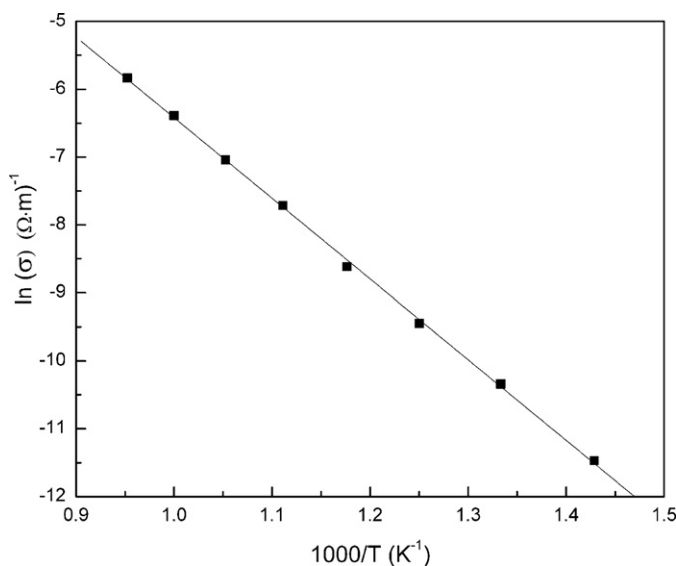

Fig. 9. Arrhenius plots of ohmic conductivity of BBiT ceramics.

ohmic conductivity was fitted according to the Arrhenius equation:

$$\sigma = \sigma_0 \exp\left(\frac{-E_a}{kT}\right), \tag{5}$$

where σ_0 is the pre-exponential factor, E_a is the activation energy per charge carrier (assumed energy required to create and move defects), k is Boltzmann's constant and T is the absolute temperature. The conductivity data follow the Arrhenius law quite well in temperature regions 700–1050 K. The calculated values of activation energy E_a, by linear fitting of the data points is 1.02 eV. The Arrhenius plot of ohmic conductivity of the samples is shown in Fig. 9. The value of E_a for conduction suggested a possibility that the conduction in the high-temperature range was ionic due to oxygen vacancies.

4. Conclusions

BBiT powders were prepared via a non-conventional solid-state reaction route based on mechanochemical synthesis during intensive milling and low temperature/time calcination step. In comparison to the literature data, such novel procedure signifi-

cantly reduced the time and temperature of calcination which leads to a considerable saving of energy and time.

X-ray diffraction pattern of BBiT ceramics can be well fitted to a tetragonal structure and indexed to a bismuth-layered perovskite structure with $n = 4$. The microstructure of BBiT ceramics indicated plate like grains with random orientation of plate faces.

The dielectric studies showed a broad dielectric anomaly with frequency dependent maximum temperature. The dielectric relaxation rate followed the empirical Vogel–Fulcher law that suggested the relaxor nature of BBiT ceramics.

The complex impedance plot exhibited one impedance semicircle identified over the frequency range of 1.21 kHz–1 MHz, which is explained by the grain effect of the bulk.

Acknowledgements

References

[1] B. Aurivillius, Arkiv. Kemi. 1 (54) (1950) 499–512.
[2] J. Tellier, Ph. Boullay, M. Manier, D. Mercurio, J. Solid State Chem. 177 (2004) 1829–1837.
[3] C. Miranda, M.E.V. Costa, M. Avdeev, A.L. Kholkin, J.L. Baptist, J. Eur. Ceram. Soc. 21 (2001) 1303–1306.
[4] G.C.C. da Costa, A.Z. Simoes, A. Ries, S.R. Foschini, M.A. Zaghete, J.A. Varela, Mater. Lett. 58 (2004) 1709–1714.
[5] A.J. Moulson, J.M. Herbert, Electroceramics, John Wiley & Sons Ltd., England, 2003.
[6] A.M. Bazargan, M. Naghavi, M. Mezaheri, S.K. Sadrnezhaat, Ceram. Int. 35 (2009) 1139–1144.
[7] T.B. de Queiroza, D. Mohrb, H. Eckertb, A.S.S. de Camargo, Solid State Sci. 11 (2009) 1363–1369.
[8] J. Chen, H. Fan, S. Ke, X. Chen, C. Yang, P. Fang, J. Alloys Compd. 478 (2009) 853–857.
[9] A.V. Murugan, S.C. Navale, V. Ravi, Mater. Lett. 60 (2006) 1023–1025.
[10] D. Xie, W. Pan, Mater. Lett. 57 (2003) 2970–2974.
[11] A. Chakrabati, J. Bera, T.P. Sinha, Physica B 404 (2009) 1498–1502.
[12] T. Kimura, Y. Yoshida, J. Am. Ceram. Soc. 89 (2006) 869–874.
[13] S. Kumar, K.B.R. Varma, J. Phys. D: Appl. Phys. 42 (2009) 075405.
[14] D.B. Jannet, M.E. Maaoui, J.P. Mercurio, Solid Solut. J. Electroceram. 11 (2003) 101–106.
[15] T. Kobayashi, Y. Noguchi, M. Miyayama, Jpn. J. Appl. Phys. 43 (2004) 6653–6657.
[16] T. Priyambodo, I. Hastiawan, A.R. Noviyati, Proceeding of the International Seminar on Chemistry, Jatinangor, 2008, pp. 469–472.
[17] B.D. Stojanovic, C.O. Pavia-Santos, M. Cilense, C. Jovalekic, Z.Z. Lazarevic, Mater. Res. Bull. 43 (2008) 1743–1753.

[18] K. Han, T. Ko, J. Alloys Compd. 473 (2009) 490–495.
[19] S. Hwee Ng, J.M. Xue, J. Wang, Mater. Chem. Phys. 75 (2002) 131–135.
[20] M.H. Sim, J.M. Xue, J. Wang, J. Metastab. Nanocryst. Mater. 23 (2005) 47–50.
[21] P. Ferrer, J.E. Iglesias, A. Castro, Chem. Mater. 16 (2004) 1323–1329.
[22] P. Ferrer, M. Alguero, A. Castro, J. Alloys Compd. 464 (2008) 252–258.
[23] Z.Ž. Lazatrević, N.Ž. Romčević, J.D. Bobić, M.J. Dohčević-Mitrović, B.D. Stojanović, J. Alloys Compd. 486 (2009) 848–885.
[24] Z.Ž. Lazatrević, J.D. Bobić, N.Ž. Romčević, N. Paunovic, B.D. Stojanović, Sci. Sinter. 41 (2009) 329–335.
[25] B.D. Stojanovic, A.Z. Simoes, C.O. Paiva-Santos, C. Jovalekic, V.V. Mitic, J.A. Varela, J. Eur. Ceram. Soc. 25 (2005) 1985–1989.
[26] B.J. Kennedy, Y. Kubota, B.A. Hunter, Ismunandar, K. Kato, Solid State Commun. 126 (2003) 653–658.
[27] B.J. Kennedy, Q. Zhou, Ismunandar, Y. Kubota, K. Kato, J. Solid State Chem. 181 (2008) 1377–1386.
[28] S.M. Pilgrim, A.E. Sutherland, S.R. Winzer, J. Am. Ceram. Soc. 73 (1990) 3122–3125.
[29] M. Correa, A. Kumar, R.S. Katiyar, Appl. Phys. Lett. 91 (2007) 082905.
[30] S.K. Kim, M. Miyayama, H. Yanagida, Mater. Res. Bull. 31 (1996) 121.